Hindawi
Geofluids
Volume 2022, Article ID 5852119, 13 pages
https://doi.org/10.1155/2022/5852119

Research Article

Spatial Characteristics and Genesis of Tight Clastic Reservoirs in Yingcheng Formation of Changling Fault Depression in the Southern Songliao Basin

Hansheng Mu,[1] Ruilei Li,[1] Jianfeng Zhu,[1] Wen Xu,[1] and Xiyu Qu[2]

[1]*Sinopec Northeast Oil and Gas Branch, Changchun, Jilin 130062, China*
[2]*School of Geosciences, China University of Petroleum, Qingdao, Shandong 266580, China*

Correspondence should be addressed to Xiyu Qu; 631505010118@mails.cqjtu.edu.cn

Received 11 July 2022; Revised 8 September 2022; Accepted 16 September 2022; Published 29 September 2022

Academic Editor: Dengke Liu

Tight oil and gas has become a hot spot for unconventional oil and gas exploration. How to find high-quality reservoirs under the conditions of low porosity and permeability has become a key issue restricting tight oil and gas exploration. This paper takes the deep-seated tight clastic rocks in the Changling fault depression in the Songliao Basin as the research object and comprehensively applies various technologies and methods such as microscopic observation, temperature measurement of inclusions and paleopressure recovery, and water-rock simulation experiments, to summarize the storage of tight reservoirs. Set space types and analyze their formation mechanism. The research results show that (1) the tight clastic reservoir space types of Yingcheng Formation in the Longfengshan subsag of the Changling fault depression in the southern Songliao Basin include residual primary pores, secondary dissolved pores, and microfractures, with mainly secondary dissolved pores; (2) pore lining chlorite is an important mechanism for the preservation of primary pores; (3) water-rock simulation experiments have confirmed that volcanic rock cuttings are easy to dissolve and are the main contributor to the secondary dissolution pores in the study area; and (4) the Raman displacement technique of methane inclusions has confirmed the existence of overpressure, which is the cause of hydrocarbon generation and pressurization and is the main motivation for a microcrack formation.

1. Introduction

Oil and gas exploration and development practices at home and abroad have confirmed that tight sandstone oil and gas is the most potential exploration direction in unconventional oil and gas, and it has become a hot research field in the global unconventional oil and gas exploration and development [1–4]. Tight reservoirs generally have the characteristics of low porosity, low permeability, low abundance and strong heterogeneity, and large changes in the distribution of sand bodies [5]. The physical characteristics of tight sandstones are the most concerned in the process of oil and gas exploration and development [6]. Previous studies on the physical properties of tight sandstone reservoirs mainly focused on the influencing factors of physical property distribution and evolution. Research on the characteristics and genetic mechanisms of relatively "high porosity and high permeability" reservoirs developed under low porosity and low permeability conditions has been intensified. It has gradually formed a consensus that sedimentation and diagenesis are the key factors affecting the physical properties of the reservoir [7–10]. However, how to find high-quality reservoirs on the background of low porosity, low permeability, low abundance, and strong heterogeneity, clarify the main controlling factors for the formation of high-quality reservoirs, and screen relatively enriched blocks (sweet spots) that are still tight. The key points and difficulties of gas exploration are discussed in this study [5]. In recent years, breakthroughs have been made in the exploration of tight gas in the Changling fault depression in the Songliao Basin. The Yingcheng Formation in the B210, B220, and B5 well areas have successively obtained tight

gas with industrial productivity and stable production. Reservoir space types and control factors are currently urgent issues that need to be resolved, and they are also an important basis for the next exploration direction selection. Based on this, this article takes the tight glutenite of the Yingcheng Formation in the Longfengshan subsag of the Changling fault depression as the research object, with the aid of polarizing microscope, scanning electron microscope, image analysis, water and rock simulation experiment, inclusion temperature measurement and paleopressure recovery, and other methods and technologies. The type of storage space in the study area and its controlling factors have been studied in detail.

2. Materials and Methods

2.1. Geological Background. The Longfengshan subsag is located in the southern part of the central depression area of the Songliao Basin, adjacent to the Darhan fault zone in the north, Changfatun uplift in the south, Beizheng fault zone in the west, and Dongling fault zone in the east, with an area of nearly 300 km^2 (Figure 1). Regionally, it is affected by the extensional strike-slip action of the Beizhengzhen fault zone and the Dongling fault zone, and the fault activity is strong.

The Lower Cretaceous strata of Longfengshan subsag are developed from bottom to top with Shahezi Formation, Yingcheng Formation, Denglouku Formation, and Quantou Formation. The lithology is mainly fine sandstone, mudstone, and glutenite. Basalt is developed in the second member of Yingcheng Formation. The Upper Cretaceous strata are developed from bottom to top with Qingshankou Formation, Yaojia Formation, Nenjiang Formation, etc. The lithology is mainly siltstone and mudstone, while the Nenjiang Formation develops a small section of dark shale.

The target horizon of this study is the Lower Cretaceous Yingcheng Formation, with fan deltas, braided river deltas, shallow lakes, and semideep lake deposits, and the overall appearance is a delta sedimentary environment with strong hydrodynamics. The grain size distribution is wide, with medium-fine conglomerate, glutenite, medium-coarse sandstone, fine-siltstone, and mudstone developed [13], which can be divided into 7 sand groups from top to bottom, of which in Ying II, the stratigraphic lithology of the section is mainly volcanic rock (andesite, basalt, etc.), fine sandstone, siltstone, and mudstone, which are volcanic caprocks [14, 15]. In Ying III sand group and Ying IV sand group, the Yingcheng Formation and Yingcheng Formation are the main gas producing zones in the study area, and the lithology is mostly glutenite. The bottom of the Yingcheng Formation is in pseudoconformity contact with the Shahezi Formation, and the top is weathered and denuded to varying degrees, and it is in unconformity contact with the bottom of the Denglouku Formation [16].

3. Results and Discussion

3.1. Reservoir Physical Properties and Storage Space Characteristics

3.1.1. Reservoir Physical Characteristics. The reservoir properties of the Yingcheng Formation in the Longfengshan subsag are poor (Figure 2). The measured porosity is mainly distributed in 3-6%. There are some high-quality reservoirs with porosity greater than 8%, with an average porosity of 4.16%; the permeability was measured. The rate is concentratedly distributed below $0.1 \times 10^{-3}\ \mu m^2$, only individual data is larger than $1 \times 10^{-3}\ \mu m^2$, and the average permeability is $0.68 \times 10^{-3}\ \mu m^2$. The measured permeability is generally an order of magnitude smaller than the overburden permeability, so the permeability of the study area is less than $0.1 \times 10^{-3}\ \mu m^2$. Refer to the Petroleum and Natural Gas Industry Standard of the People's Republic of China-Tight Sandstone Gas Geological Evaluation Method (SY/T 6832-2011). The area is a typical tight gas reservoir.

3.1.2. Reservoir Space Characteristics. The storage space types of tight clastic reservoirs in the Yingcheng Formation of the Longfengshan subsag include residual primary pores, secondary dissolved pores, and microfractures. Residual primary pores account for about 38.2% of the total aperture ratio, secondary dissolution pores account for about 60.3% of the total aperture ratio, and microcracks account for about 1.5% of the total aperture ratio.

3.1.3. Residual Primary Pores. The primary pores in the tight clastic reservoirs of the Yingcheng Formation in the Longfengshan subsag are dominated by primary residual intergranular pores. The pores are of relatively regular shape and are mostly surrounded by pore lining chlorite. There is a certain amount of microcrystalline quartz in the pores (Figures 3(a) and 3(b)). Pore lining chlorite grows like a crustacean around the pores, with a thickness of about 5-15 μm. The chlorite in the pore lining where the particles contact is basically not developed, and the chlorite crystals are leaf-shaped. The existence of primary residual intergranular pores may be related to the development of chlorite lining the pores.

3.1.4. Secondary Dissolution Pores. The secondary pores in the tight clastic reservoirs of the Yingcheng Formation in the Longfengshan subsag are mainly produced by dissolution and can be divided into intergranular dissolution pores, intragranular dissolution pores, and mold pores. The intragranular dissolved pores in the study area are mainly formed by intragranular dissolution of volcanic rock debris, mainly composed of intragranular dissolved pores in andesite rock debris (Figure 4(a)) and intragranular dissolved pores in acid erupted rock debris (Figure 4(b)); intragranular dissolved pores in feldspar are the second (Figure 4(c)); a small amount of quartz is also developed. Dissolved pores within the grains (Figure 4(d)) and mold pores (Figure 4(e)) are present; the dissolved pores between grains are mainly the dissolution pores of laumontite cement (Figure 4(f)). The dissolved pores in the andesite rock fragments are mostly honeycomb-shaped micropores with irregular shapes, which can provide material sources for the formation of iron-bearing cements such as chlorite (Figure 4(a)). When the dissolution is strong, the mold pores can be formed (Figure 4(b)); the intragranular dissolution of feldspar and quartz particles usually form larger regular dissolution pores,

activity is strong.

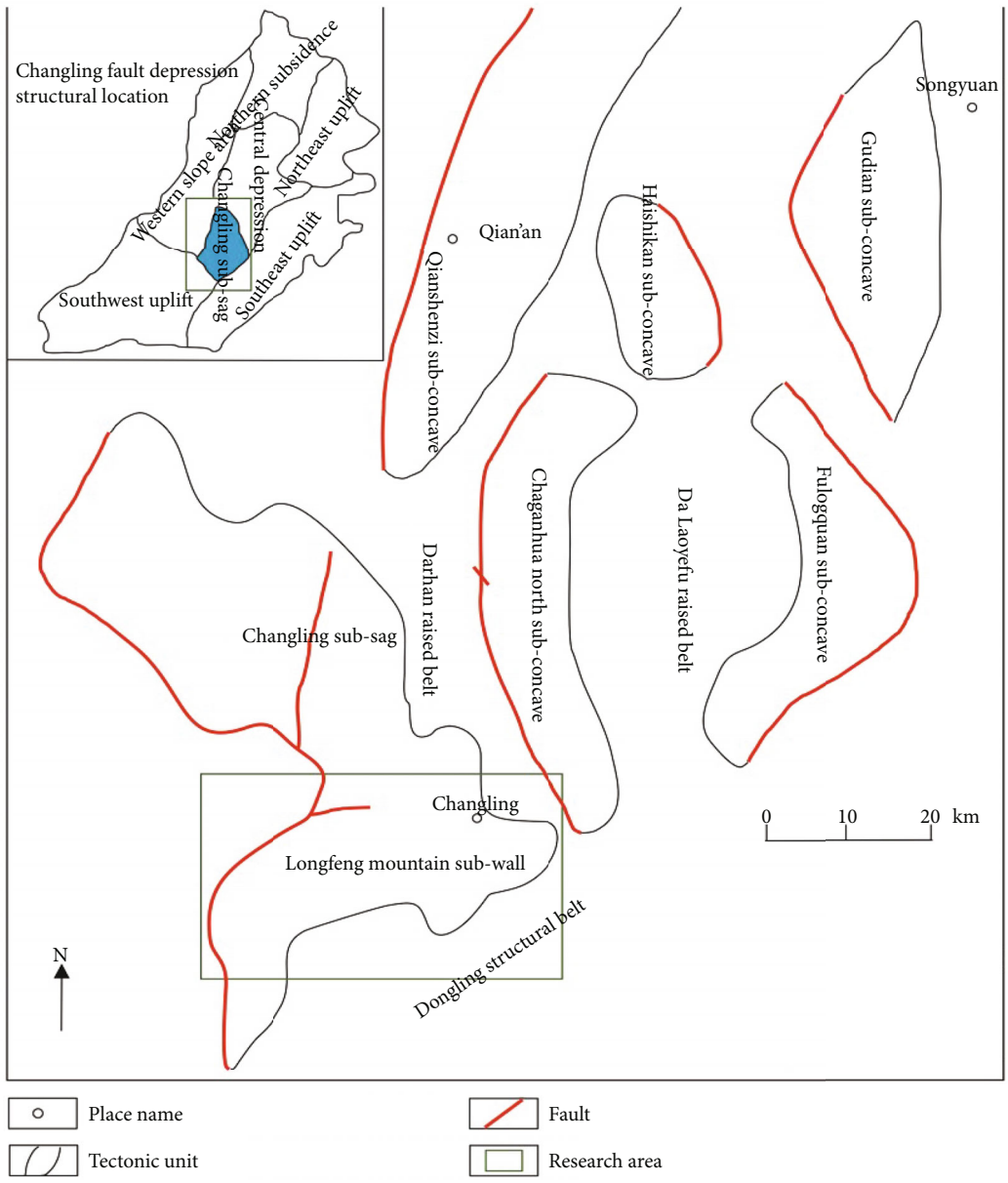

(a)

Figure 1: Continued.

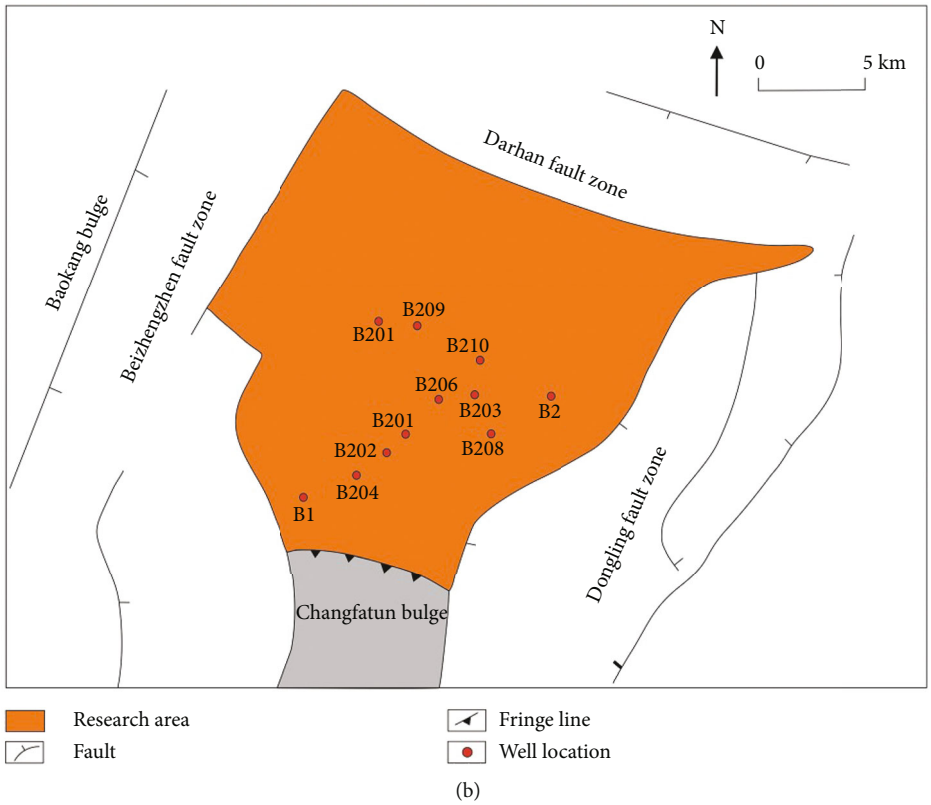

Figure 1: Longfengshan subsag structure location (a) and well location distribution map (b) [11, 12].

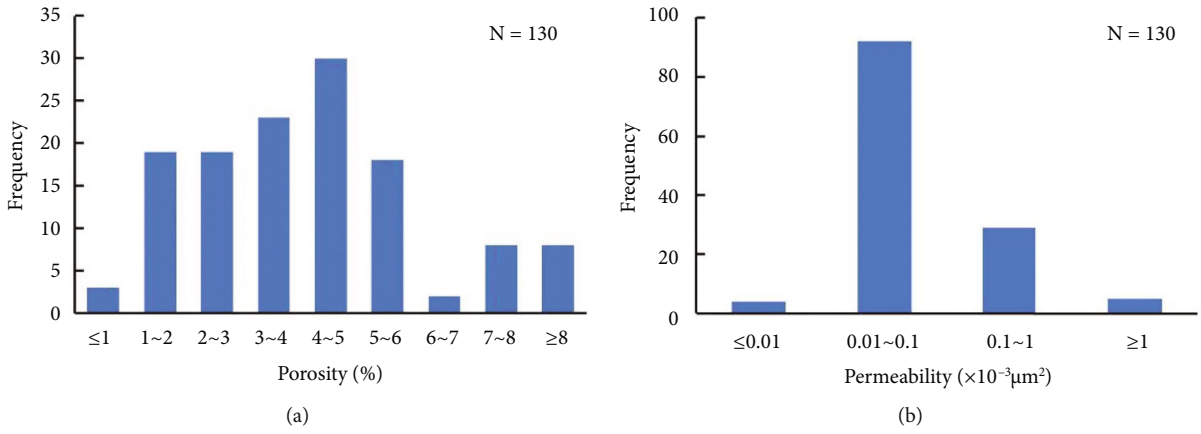

Figure 2: Distribution histograms of porosity (a) and permeability (b) of clastic reservoirs in Yingcheng Formation in the study area.

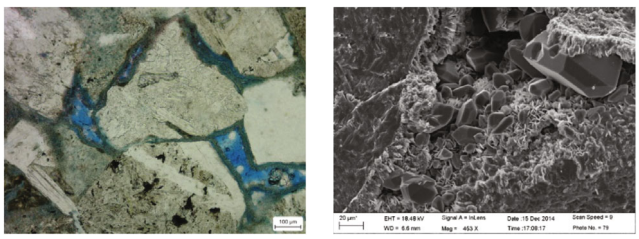

Figure 3: (a) Porous lining chlorite surrounds the intergranular pores, and the pores are filled with microcrystalline quartz, B202 well, 3117.80 m (-). (b) Porous lining chlorite surrounds the intergranular pores, and the pores are filled with microcrystalline quartz, B202 well, 3098.9 m, SEM.

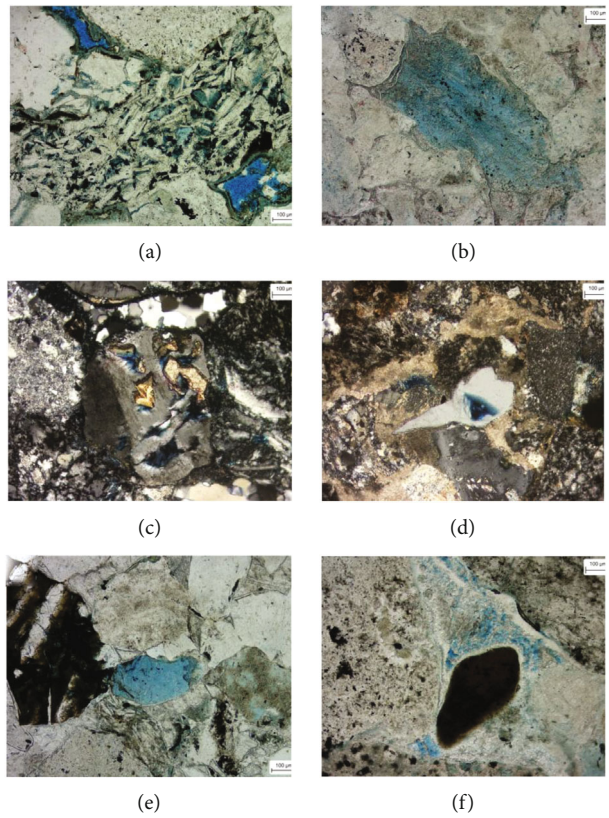

Figure 4: (a) Dissolved pores in the andesite cuttings, the pores are lined with chlorite to surround the intergranular pores, and the pores are filled with microcrystalline quartz, well B202, 3112.75 m (-). (b) Acid erupted rock cuttings dissolve to form mold holes, well B210, 3948.60 m (-). (c) Feldspar pores, B210 well, 3950.9 m (+). (d) Quartz pores, B210 well, 4129.95 m (+). (e) mold hole, B202 well, 3130.8 m (-). (f) Lautonite cement dissolution pores, well B210, 3945.95 m (-).

and the edge dissolution usually forms bay-like dissolution pores (Figures 4(c) and 4(d)). The dissolution of lautonite cleavage cracks expands (Figure 4(f)).

According to the statistics of the hole ratio of the secondary dissolved pores in the study area, it is found that the intragranular dissolved pores in the volcanic rock fragments account for 72.50% of the secondary pore surface ratio, and the intergranular dissolved pores account for 22.10%, indicating that the secondary dissolved pores are mainly composed of volcanic rock. Provided by dissolution in crumbs.

3.2. Microcracks. There are a certain number of microfractures in the tight clastic reservoirs of the Yingcheng Formation in the Longfengshan subsag, mainly in the form of bonded-grain fractures (Figure 5(a)) and envelope fractures (Figure 5(b)), and a small number of them are structural fractures (Figure 5(c)). It can also be seen that dissolution expansion (Figure 5(d)) and organic matter filling occur along the microfractures (Figure 5(e)). Image analysis with cast thin slices as the statistical unit shows (Table 1) that the average width of microcracks is 2.5 μm; the average number of cracks in the thin slices is about 5, up to 36. The more developed position of the fracture corresponds to the high value of permeability. For example, B210 well develops glued fractures at 3945.95 m and 3947.5 m, and the permeability is $6.389 \times 10^{-3}\ \mu m^2$ and $4.59 \times 10^{-3}\ \mu m^2$, respectively; another example is B206 well 3243.61. The fractures at m are very developed, and the permeability is as high as $11.4 \times 10^{-3}\ \mu m^2$, indicating that the existence of microfractures improves the permeability of the reservoir.

3.3. The Formation Mechanism of the Reservoir Space

3.3.1. Pore Lining Chlorite Is the Main Reason for Primary Pore Protection

(1) The Relationship between Pore Lining Chlorite and Primary Pores. Pore lining chlorite is often formed in a weakly alkaline (pH 7-9) reducing environment rich in iron and magnesium [17–19]. It is formed earlier and mainly protects the quality of the reservoir. For example, in well B202 3093 m and 3093 m, the content of authigenic chlorite at 3099 m reached high values of 6.8% and 5.9%, respectively, and the corresponding porosity and permeability also reached the maximum at this depth. The maximum porosity was 8.8%, and the maximum permeability was 0.357 mD (Figure 6). It shows that there is a positive correlation between the content of authigenic chlorite and porosity, and the higher the content of chlorite in the pore lining, the better the protective effect on the physical properties of the reservoir.

The statistical results of the porosity and primary residual intergranular porosity of the samples with more

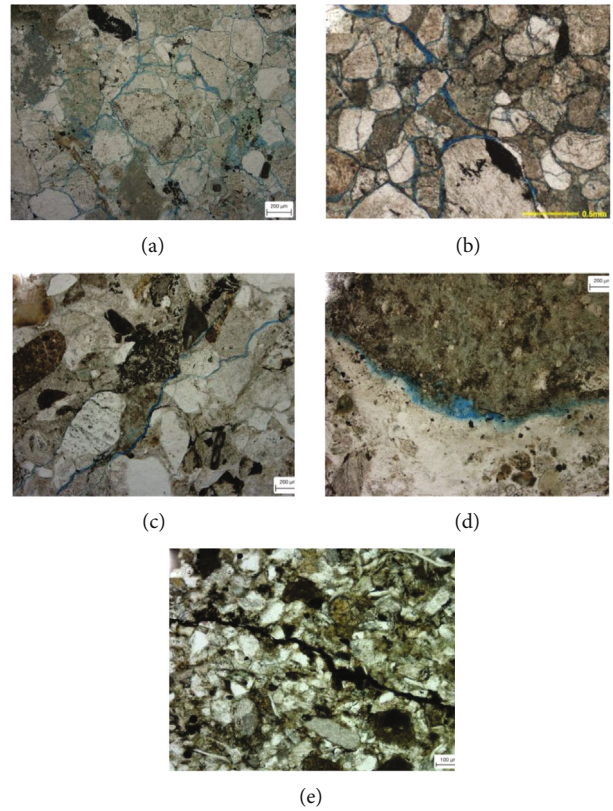

(a) (b) (c) (d) (e)

Figure 5: (a) Grained fractures, well B206, 3243.61 m (-). (b) Enveloping fractures, B210 wells, 3945.08 m (-). (c) Structural fractures, B208 wells, 3261.45 m (-). (d) Grained fracture dissolution, well B210, 4127.2 m (-). (e) Fracture is filled with organic matter, well B203, 3607.8 m (-).

Table 1: Statistical table of microcrack image analysis results.

No.	Depth (m)	Number of cracks (pieces)	Average crack opening (μm)	Crack density (mm/mm^2)
B201	3398.01	3	2.5	0.62
B202	2994	5	2.5	0.66
B202	2998.75	4	2.5	0.83
B202	3087.33	11	2.5	1.39
B202	3098.9	3	2.5	1.44
B202	3128.6	3	2.5	0.65
B203	3317.87	6	2.5	0.5
B204	2389.4	4	2.5	0.94
B204	2875.4	5	2.5	0.9
B206	3237.22	9	3.62	0.28
B206	3237.58	5	2.5	1.92
B206	3243.61	36	5.99	1.33
B210	3945.03	12	2.89	1.13
B210	3945.95	4	2.5	0.08
B210	3947.5	8	2.5	0.87
B210	3950.9	12	2.6	2.5
B210	3951.65	5	2.5	0.99

developed pore lining chlorite show that the total porosity of the sample is 5.06%-8.66%, the primary residual intergranular porosity is 3.62%-6.29%, and the ratio of primary porosity to the total porosity is 53.31%-83.60%, with an average of 65%, indicating that the porosity of the sample is mainly provided by the residual intergranular pores (Table 2), and

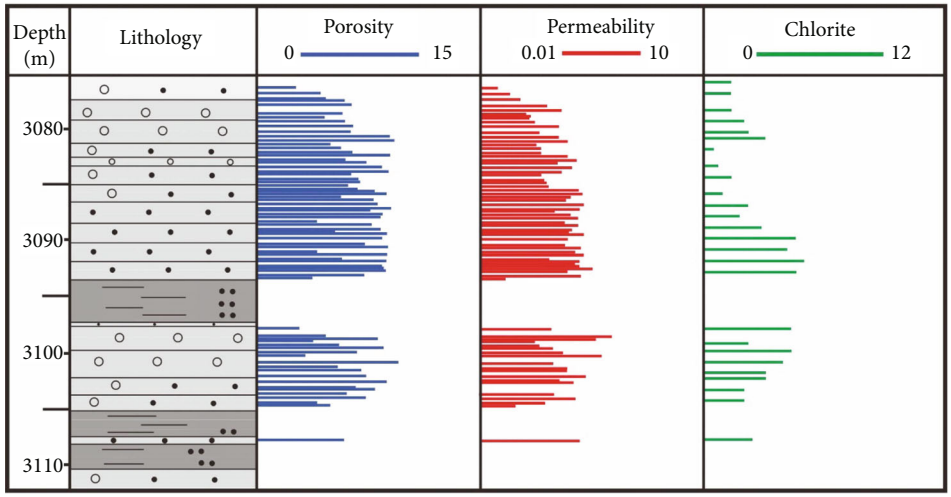

Figure 6: The relationship between porosity, permeability, and chlorite content in the core section of well B202.

Table 2: Statistical table of the hole ratio of the chlorite development section in the pore lining of well B202.

No.	Depth (m)	Porosity (%)	Total area porosity (%)	Hole area ratio between residual particles (%)	Proportion of primary pore surface porosity (%)
B202	2994	7.57	6.15	4.05	65.85
	2998.75	5.60	5.06	4.23	83.60
	3087.33	8.18	6.79	3.62	53.31
	3098.9	8.75	6.88	3.71	53.92
	3112.75	8.2	6.82	4.03	59.09
	3117.8	7.92	6.49	4.32	66.56
	3128.6	10.26	8.66	6.29	72.63

the primary porosity is relatively large. Pore lining chlorite protects porosity mainly in the preservation of primary pores (Figure 7).

(2) Pore Preservation Mechanism of Chlorite in Pore Lining. Pore lining chlorite protects the primary pores in the study area mainly in the following aspects:

(1) Slow down the compaction effect. In the thin slices with chlorite lining the pores in the study area, the contact relationship between the particles is weak, mainly point-line contact (Figure 8). Pore lining chlorite was formed in the early diagenesis period. The alteration of early dark minerals and the dissolution of volcanic rock cuttings provided a rich source of iron for the formation of pore lining chlorite in the study area. Pore lining chlorite formed earlier, and the formation period was earlier than that of microcrystalline quartz and carbonate cement. At this time, the reservoir has not undergone strong compaction and cementation, and the pore lining chlorite occupies a certain space. It can effectively slow down the compaction effect, which is conducive to the preservation of primary pores [19]

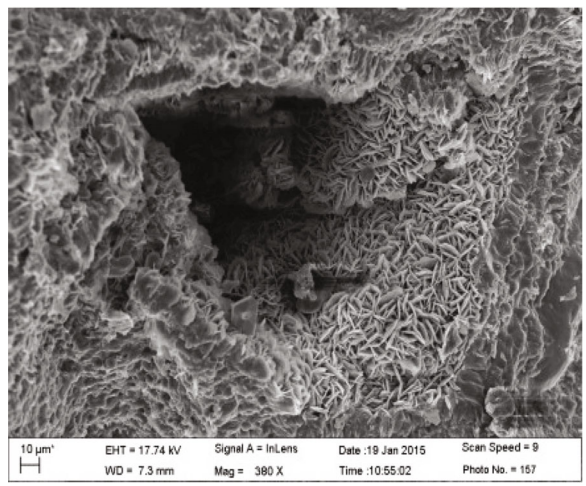

Figure 7: Pore lining primary pores surrounded by chlorite, well B202, 3096.25 m, SEM.

(2) Suppress the secondary growth of quartz. Because the pore lining chlorite can slow down a certain degree of compaction, the contact between particles

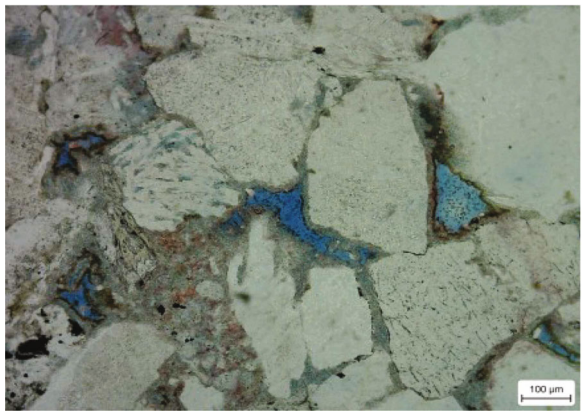

Figure 8: Pore lining chlorite surrounds the remaining intergranular pores, well B202, 3128.6 m (-).

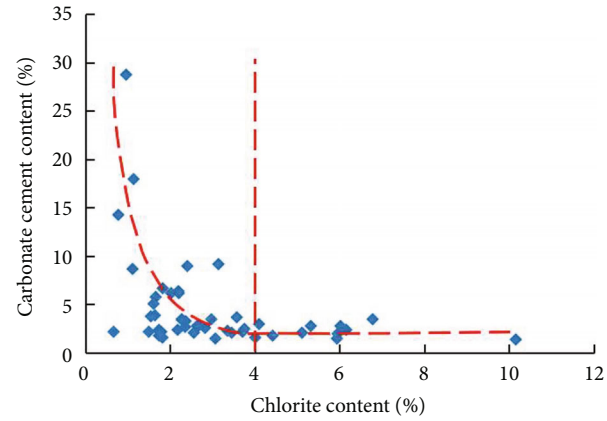

Figure 9: The relationship between chlorite content and carbonate cement content in the study area.

is weak, and it can inhibit the pressure dissolution of quartz to a certain extent, reduce the content of SiO_2 in the pore fluid, and reduce the substance of secondary quartz source. In addition, the pore lining chlorite adheres to the surface of the quartz particles, which makes the contact surface between the quartz particles and the pore fluid smaller, and it is difficult for the SiO_2-rich fluid to nucleate on the quartz surface, which inhibits the secondary growth of quartz [20]. Therefore, in reservoirs with well-developed pore lining chlorite, there is no secondary enlargement of quartz, and siliceous cements mostly exist in the intergranular pores in the form of authigenic microcrystalline quartz (Figure 3)

(3) Inhibit carbonate cementation. Pore lining chlorite is mainly formed in a high-energy, open, weakly alkaline, and weakly reducing environment and mainly developed in the subfacies underwater distributary channel microfacies of the delta front [19]. Underwater distributary channels have strong microphase hydrodynamic conditions and active pore fluid migration. Under the pressure generated by the local flow velocity on the particle surface, clay adsorbs on the particle surface to form pore lining chlorite [21], which can inhibit carbonate cementation. The content of chlorite in the study area is obviously negatively correlated with the content of carbonate cement (Figure 9). When the chlorite content is less than 4%, with the increase of the chlorite content, the carbonate cement content decreases obviously; when the chlorite content is greater than 4%, the carbonate cement content increases with the increase of the chlorite content. The cement content did not change much

3.4. The Dissolution of Volcanic Rock Debris Is the Main Contributor to Secondary Dissolution Pores

3.4.1. Types of Cuttings and Their Relationship with Pores. The sandstone of the Yingcheng Formation in the Longfengshan subsag is mostly lithic sandstone (Figure 10), and the average ratio of lithic, feldspar, and quartz is 67 : 19 : 14. The types of cuttings are mainly volcanic rock cuttings (basalt, andesite, and acidic eruption rock), accounting for about 40.00%, and the highest is 55.30% (Table 3). Among them, acidic erupting rock cuttings and andesite cuttings have the most content and acidic eruption. The average content of rock cuttings is 22.52%, and the average content of andesite cuttings is 14.66%. Dissolved pores in volcanic rock cuttings account for 72.50% of the secondary pores, and they are the main contributor to the secondary dissolved pores.

3.4.2. Discussion on the Formation Mechanism of Lithic Dissolution Porosity. In order to explore the contribution of the dissolution of different types of cuttings to the generation pores of the reservoir, five groups of high-content cuttings (rhyolite, andesite, basalt, gneiss, and schist) in the study area were designed. The samples are fresh andesite, rhyolite, basalt, gneiss, and schist on the surface. Before the experiment, the sample was ground into a rectangular parallelepiped of $1\,cm \times 1\,cm \times 0.8\,cm$, and the surface was polished. The organic acid solution used in the experiment was prepared according to the type and quantity of the existing type II1 kerogen discharged organic acid. The specific preparation process was consistent with the literature [22], and the pH of the solution was 3.71. Three temperature conditions of 100°C, 150°C, and 200°C were selected for the experiment temperature, and the formation temperature of 2500 m, 3500 m, and 4500 m was simulated, respectively. Since the pressure has a small effect on the dissolution, the experimental pressure is uniformly selected as 30 MPa.

The experimental device is a KDSF-II high-temperature and high-pressure reactor. The specific experimental steps are as follows: (1) put the sample into the hanging basket in the reactor, pour the prepared organic acid solution, and seal the reactor; (2) set the experimental temperature, fill the kettle with N_2 to make the pressure in the kettle reach about 25 MPa, turn on the heating button to slowly raise the temperature of the reaction kettle, and continue to fill the kettle with a small amount of N_2 after reaching the target temperature to make the pressure reach 30 MPa; (3) keep constant temperature and pressure conditions to react 48 h;

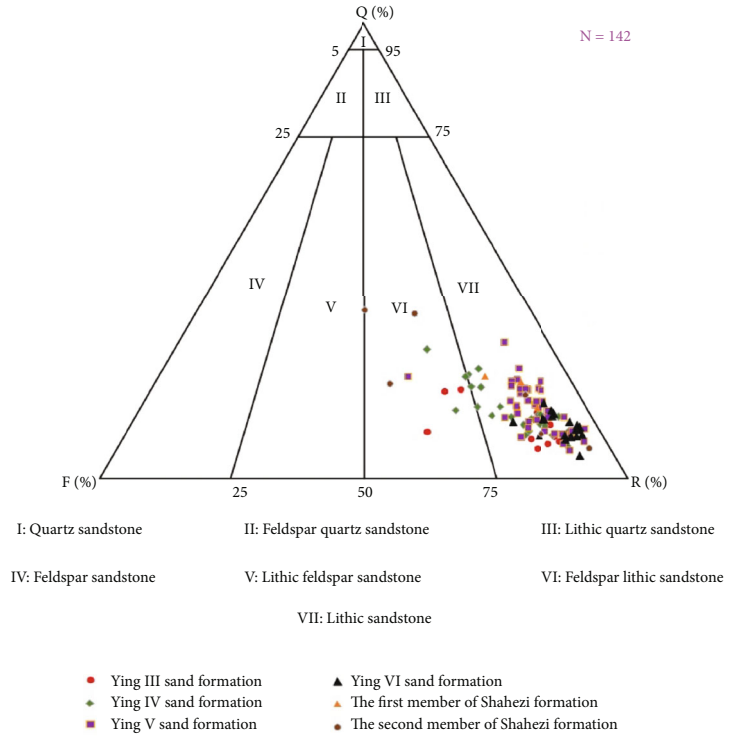

Figure 10: Triangular diagram of the sandstone classification of the Yingcheng and Shahezi formations in the study area.

Table 3: Statistics of cuttings types and content in the study area.

No.	Magmatic rock debris				Metamorphic rock cuttings				
	Andesite	Acid extrusive rock	Basalt	Granite	Quartzite	Schist	Gneiss	Phyllite	Slate rock
B201	20.1	25.2	3.0	1.0	7.9	8.8	1.7	0.6	1.3
B202	21.6	24.6	2.4	1.7	7	7.9	3.1	1.4	1.8
B203	15.2	17.5	2.1	1.3	5.2	12.2	1.8	0.8	2.6
B204	15.5	35.3	4.5	1.5	6.6	10.0	3.2	0.8	2.1
B206	13.4	21.1	2.5	2.1	13.4	7.7	3.1	2.1	1.4
B208	7.9	17.6	2.1	0.0	15.7	4.7	3.0	1.0	1.3
B209	16.1	26.1	3.1	0.9	9.0	5.6	1.4	1.1	1.0
B210	25.1	14.8	2.0	1.3	17.6	3.4	5.4	1.5	1.2
B211	8.7	26.0	1.3	3.0	15	15.0	10.0	5.0	0.0
B2	3.0	17.0	1.0	0.0	1.0	2.0	0.0	0.0	0.0

(4) after the experiment, power off and let it cool naturally. When the temperature in the kettle drops to room temperature, take out the sample, wash and dry and weigh it, take out the reaction solution with a disposable syringe, and check the ion concentration.

According to the mass loss before and after the reaction (Figure 6), the mass loss percentage of basalt, rhyolite, and andesite at 100°C is between 0.97% and 1.74%, while the mass loss of gneiss and schist is less, ranging from 0% to 0.9%. When the temperature is 150°C, the percentage of mass loss of basalt, rhyolite, and andesite is about 1.05%~1.42%, and that of gneiss and schist is about 0%~1%, and the degree of mass loss is close to that at 100°C. When the temperature is 200°C, the percentage of mass loss of basalt, rhyolite, and andesite is about 1.36%~2.45%, while that of gneiss and schist is only 0.52%~0.87%. From the perspective of the pH change of the solution before and after the reaction (Figure 11), the pH of the solution before and after the reaction of basalt, rhyolite, and andesite changed greatly, and the pH value of the solution before and after the reaction of gneiss and schist was small, indicating that the basalt, flow laminite, and andesite are more soluble in acidic conditions.

The mass loss percentage, pH, and total ion concentration before and after the comprehensive reaction are shown in Figure 11. The mass loss percentage, pH value, and total ion concentration of basalt, rhyolite, and andesite before and after the reaction have changed greatly, and the gneiss

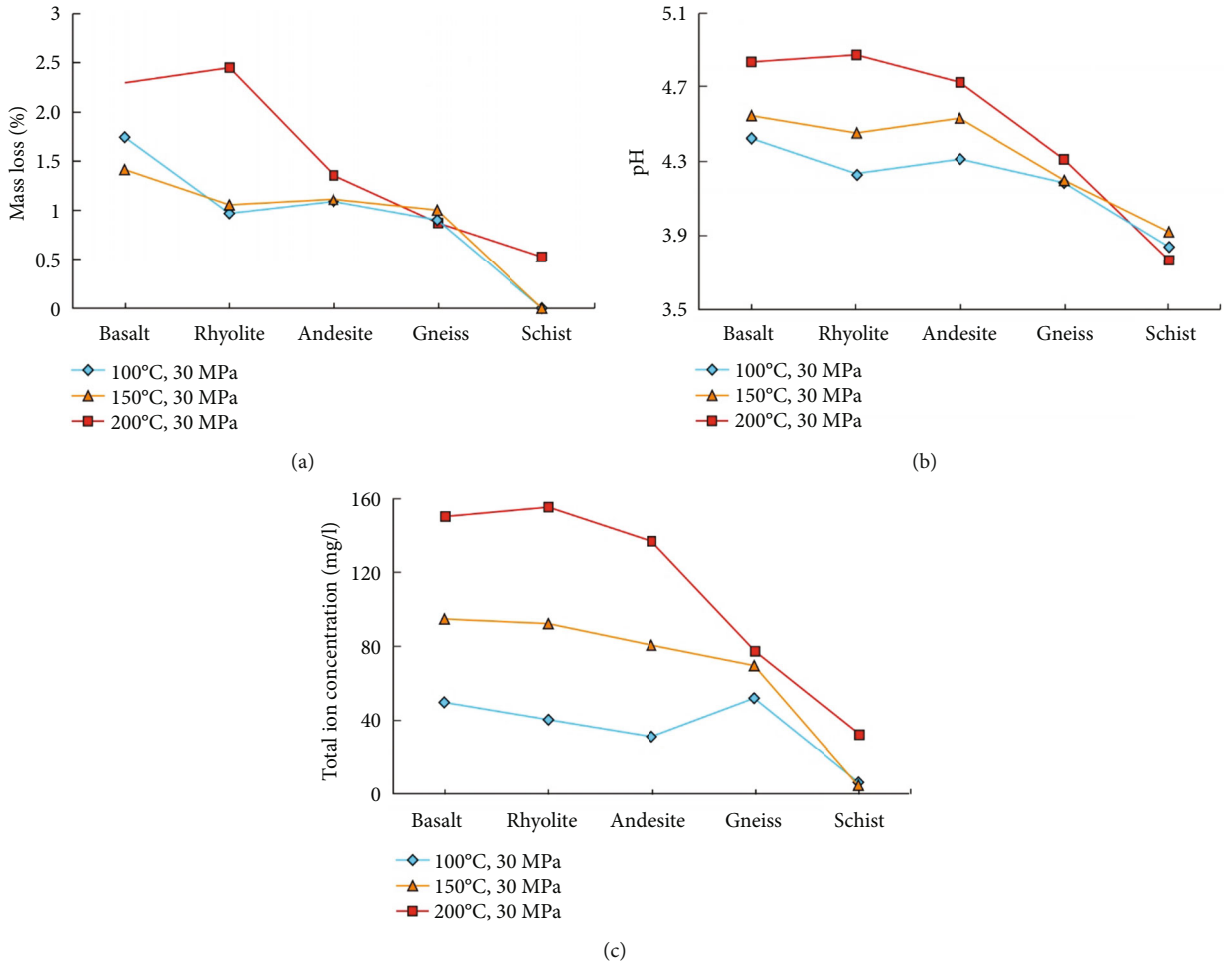

Figure 11: The percentage of mass loss, pH, and total ion concentration of different types of cuttings under different temperature and pressure conditions. (a) Percentage of mass loss, (b) pH, and (c) total ion concentration.

Table 4: Measured and calculated data table of methane inclusions in the well section with microfractures.

No.	Depth (m)	Stratum	Homogenization temperature of inclusions (°C)	Methane inclusion density (g/cm^3)	Capture pressure (MPa)
B206	3234.89	Ying III sand formation	110	0.24	62.86
B210	3945.33	Ying VI sand formation	130	0.24	68.74
B210	4129.65	Ying VI sand formation	130	0.24	68.74

and schist have changed smaller. On the whole, rhyolite is the most soluble, followed by basalt and andesite, and gneiss and schist have poor dissolution. The content of volcanic rock debris in the study area is the highest, of which rhyolite debris content is the largest, followed by andesite debris, indicating that volcanic rock debris is the main contributor to the secondary pores in the study area.

3.5. Hydrocarbon Generation Pressurization Is the Main Driving Force for the Formation of Microfractures

3.5.1. Paleopressure Recovery of Inclusions. There is an obvious correlation between the Raman displacement value of gaseous methane inclusions and its internal pressure, and the Raman displacement value of methane inclusions decreases with the increase of pressure. Using this feature, the equation of state for methane inclusions can be established. This time, the methane equation of state is used to calculate the trapping pressure of methane inclusions [23], and then, the ancient pressure of the formation can be restored.

The methane inclusion density of the sample is obtained from the characteristic peak of methane Raman scattering, and then, the trapping pressure of the methane inclusions is obtained. The uniform temperature and capture pressure of methane inclusions are shown in Table 4. The capture pressure is above 60 MPa, and the highest is 68.74 MPa,

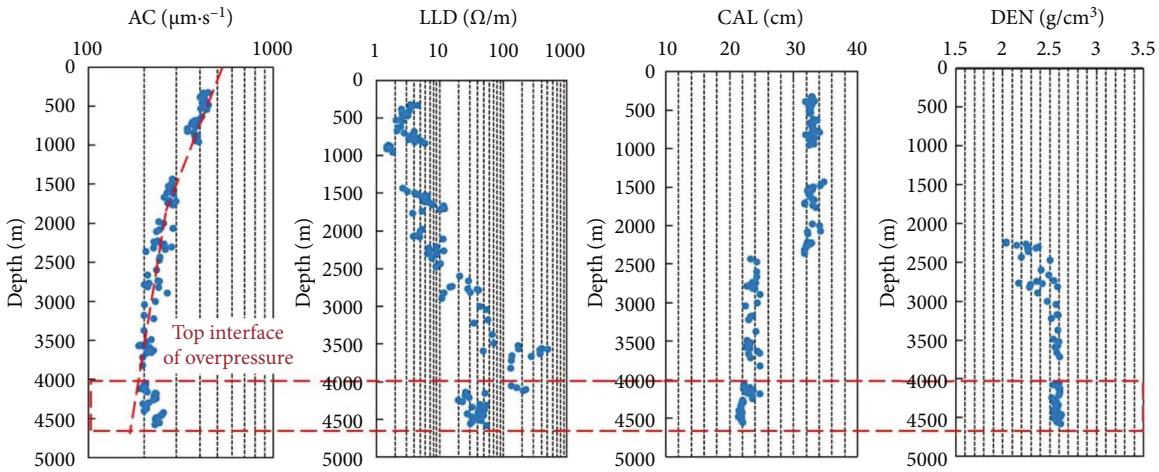

Figure 12: Curves of acoustic time difference, resistivity, well diameter, and density of mudstone in well B212.

indicating that there was abnormal high pressure in the formation during this period.

3.5.2. Log Identification of Overpressure. The mudstone acoustic time difference curve of well B212 deviates from the normal trend at about 4000 m, indicating that 4000 m is the overpressure top interface of well B212. Below 4000 m, the sonic time difference increases abnormally, while the density is basically unchanged (Figure 12), indicating that the overpressure is not the cause of undercompaction but may be the cause of hydrocarbon generation and pressurization.

The mudstone acoustic time difference-density intersection diagram of well B212 is shown in Figure 13. The point on the curve is the average value of the acoustic velocity and density of the mudstone section. The mudstone section has a normal well diameter (to ensure that there is no well diameter expansion section), the mud content is greater than or equal to 90%, and the thickness is greater than 2 m (to reduce the impact of surrounding rock). From the intersection diagram (Figure 13), it can be seen that the density of the overpressure section of well B212 basically remains unchanged with the decrease of the acoustic velocity, which is in line with the cause of hydrocarbon generation and pressurization in the acoustic velocity-density intersection diagram discrimination method [24].

3.5.3. Overpressure Is the Cause of Hydrocarbon Generation and Pressurization and Is the Main Driving Force for the Formation of Microfractures. The abnormal pressure of fluid generated by organic matter hydrocarbon generation is an important overpressure formation mechanism [25]. In the theory of "episodic hydrocarbon expulsion," hydrocarbon generation pressurization is the material guarantee and power source for the first migration of oil and gas [26–28]. There are two phases of oil and gas charging in the study area, corresponding to the homogenization temperature of fluid inclusions being 90°C-110°C and 120°C-140°C [29]. The matching of hydrocarbons indicates that during the duration of the two hydrocarbon generation periods, the

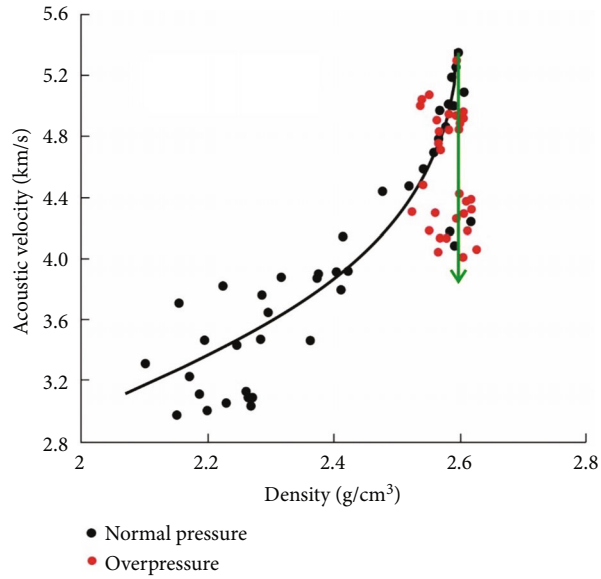

Figure 13: Sonic velocity-density intersection diagram of mudstone in well B212.

kerogen interstitial hydrocarbon expulsion caused the fluid in the pores to expand rapidly, resulting in overpressure. Combining with the logging identification results of overpressure, it can be proved that the overpressure in the study area is an increase in hydrocarbon generation. Tight reservoirs have small pore throats, high capillary resistance, and limited buoyancy migration. It has become a consensus that pressurization of hydrocarbon generation is the main driving force for the migration of oil and gas in tight reservoirs [30–32]. At the same time as the episodic expulsion of hydrocarbons and pressure to the outside, the hydrocarbons and pressure enter the reservoir together, forming a hydrocarbon-generating pressurized overpressure. When the reservoir pressure exceeds the rock fracture conditions, microfractures such as stick-grain fractures and envelope fractures will be generated. Hydrocarbon generation pressurization is the main driving

force for the development of microfractures in the study area. The microfractures formed not only connect the pores and improve the permeability of the reservoir. It also provides convenient conditions for the later fracturing construction.

Diagenesis, mineral transferring, diageneic stages, and porosity development of these sandstones should be discussed to help to understand the processes and controlling factors of disfication of the sandstone reservoirs. Limited by laboratory conditions and some objective factors, we cannot finish it. This aspect will be considered in subsequent research.

4. Conclusions

The tight clastic reservoir space types of the Yingcheng Formation in the Longfengshan subsag of the Changling fault depression in the southern Songliao Basin include residual primary pores, secondary dissolved pores, and microfractures, with mainly secondary dissolved pores.

There is a positive correlation between the content of chlorite in pore lining and porosity, which is an important mechanism for the preservation of primary pores. The chlorite lining in pores can slow down compaction, inhibit quartz secondary growth and carbonate cementation, and protect primary pores.

Water-rock simulation experiments confirmed that volcanic rock debris is easily soluble, of which rhyolite is the most soluble, followed by basalt and andesite; the study area has the highest content of volcanic debris and is dominated by rhyolite and andesite debris. Volcanic rock debris is the main contributor to secondary pores in the study area.

The Raman displacement technology of methane inclusions confirmed the existence of overpressure. Combining logging identification and hydrocarbon generation period matching relationship, it was determined that overpressure was formed by hydrocarbon generation pressurization, and this overpressure was the main driving force for the formation of microfractures.

Data Availability

The experimental data used to support the findings of this study are available from the corresponding author upon request.

Conflicts of Interest

The authors declare that they have no conflicts of interest.

Acknowledgments

This research was funded by the Key Scientific and Technological Project of China Petroleum & Chemical Corporation "Songnan Fault Depression Deep Tight Sandstone Gas Accumulation Conditions and Target Evaluation (Grant No. P20060-6)."

References

[1] S. A. Holditch, "Tight gas sands," *Journal of Petroleum Technology*, vol. 58, no. 6, pp. 86–93, 2006.

[2] S. H. Nordeng, "The Bakken petroleum system: an example of a continuous petroleum accumulation," *DMR Newsletter*, vol. 36, no. 1, pp. 21–24, 2010.

[3] W. R. Hu, J. W. Bao, and B. Hu, "Trend and progress in global oil and gas exploration," *Petroleum Exploration and Development*, vol. 40, no. 4, pp. 439–443, 2013.

[4] C. N. Zou, G. Y. Zhang, and S. Z. Tao, "Geological features, major discoveries and unconventional petroleum geology in the global petroleum exploration," *Petroleum Exploration and Development*, vol. 37, no. 2, pp. 129–145, 2010.

[5] X. J. Liu, Z. J. Ma, and D. Han, "Research on the main factors of high quality tight sandstone reservoir in Linxing block, Ordos Basin," *Natural Gas Geoscience*, vol. 29, no. 4, pp. 481–490, 2018.

[6] A. Wang, D. K. Zhong, and Z. Q. Liu, "Characteristics of deep tight sandstone reservoirs and their controlling factors of physical properties: a case study of the Xu-2 member in the western Yuanba area of the northeastern Sichuan Basin, China," *Acta Sedimentologica Sinica*, vol. 2, pp. 410–421, 2022.

[7] G. Y. Li, F. Q. Lai, and J. C. He, "Reservoir characteristic and controlling factors on physical properties of Lower Jurassic tight sandstone in the Qiudong sub-sag, Turpan-Harmi Basin," *Natural Gas Geoscience*, vol. 24, no. 2, pp. 310–319, 2013.

[8] H. H. Zhu, D. K. Zhong, and Y. X. Zhang, "Pore types and controlling factors on porosity and permeability of Upper Triassic Xujiahe tight sandstone reservoir in southern Sichuan Basin," *Oil & Gas Geology*, vol. 35, no. 1, pp. 65–76, 2014.

[9] X. Chen, X. Y. Qu, and L. W. Qiu, "Physical property of the Upper Paleozoic tight sandstone reservoir and its main controlling factors during diagenesis of well D18 in Daniudi gas field," *Acta Sedimentologica Sinica*, vol. 34, no. 2, pp. 364–374, 2016.

[10] W. X. Han, L. H. Hou, and J. L. Yao, "Characteristics and formation mechanism of Chang 7 tight sandstone reservoir in Ordos Basin," *Journal of China University of Mining & Technology*, vol. 45, no. 4, pp. 765–771, 2016.

[11] Z. X. Zuo, J. L. Lu, and M. Wang, "Fault characteristics and controls on hydrocarbon accumulation in Changling faulted depression, Songliao Basin," *Petroleum Geology Experiment*, vol. 41, no. 2, pp. 200–206, 2019.

[12] J. Yuan, W. Wang, and J. F. Zhu, "Research on provenance and sedimentary facies of Yingcheng Formation in Lower Cretaceous in Longfengshan subsag, Changling fault depression, Songliao Basin," *Natural Gas Geoscience*, vol. 28, no. 1, pp. 93–105, 2017.

[13] X. X. Liu, X. N. Zhang, and P. Yang, "Formation mechanism of deep high-quality reservoirs of Yingcheng Formation in Longfengshan area, Songliao Basin," *Lithologic Reservoirs*, vol. 29, no. 2, pp. 117–124, 2017.

[14] W. Guo, W. X. Yu, and Z. J. Liu, "The burial history of the southern Songliao Basin," *Journal of Jilin University (Earth Science Edition)*, vol. 39, no. 3, pp. 353–360, 2009.

[15] H. Li, J. L. Lu, and Z. X. Zuo, "Controlling factors of high-quality lacustrine hydrocarbon source rocks in southern Changling depression," *Oil & Gas Geology*, vol. 36, no. 2, pp. 209–218, 2015.

[16] R. H. Cheng, Y. G. Ren, and Y. J. Shen, "Volcanic cooling unit and analysis of stratigraphic architecture of Yingcheng Formation in Songliao Basin," *Journal of Jilin University (Earth Science Edition)*, vol. 42, no. 5, pp. 1338–1347, 2012.

[17] J. F. Tian, Z. L. Chen, and Y. Y. Yang, "Protection mechanism of authigenic chlorite on sandstone reservoir pores," *Geological Science and Technology Information*, vol. 27, no. 4, pp. 49–54, 2008.

[18] W. R. Xie, W. Yang, and X. Y. Zhao, "Influence of chlorite on reservoir physical properties of the Xujiahe Formation in the central part of Sichuan Basin," *Petroleum Exploration and Development*, vol. 37, no. 6, pp. 674–679, 2010.

[19] X. Y. Qu, Z. Liu, and Y. Gao, "The influence and formation environment of chlorite coatings in the clastic rock," *Acta Sedimentologica Sinica*, vol. 33, no. 4, pp. 786–794, 2015.

[20] S. J. Huang, L. W. Xie, and M. Zhang, "Formation mechanism of authigenic chlorite and relation to preservation of porosity in nonmarine Triassic reservoir sandstones, Ordos Basin and Sichuan Basin, China," *Journal of Chengdu University of Technology (Science& Technology Edition)*, vol. 3, pp. 273–281, 2004.

[21] Z. Cao, G. D. Liu, W. Meng, P. Wang, and C. Yang, "Origin of different chlorite occurrences and their effects on tight clastic reservoir porosity," *Journal of Petroleum Science and Engineering*, vol. 160, pp. 384–392, 2018.

[22] Y. Q. Cao, Q. B. Wang, and X. Y. Qu, "A dissolution experiment of organic acid of cuttings and itsverification: a case study of the Dongying Formation of the CFD6-4 oilfield, Bozhong sag," *Acta Petrolei Sinica*, vol. 41, no. 7, pp. 841–852, 2020.

[23] L. W. Wang, X. Z. Chen, and Y. J. Hou, "The study and application of equation of state of methane," *Journal of Chemical Engineering of Chinese Universities*, vol. 2, pp. 103–108, 2001.

[24] J. Z. Zhao, J. Li, and Z. Y. Xu, "Advances in the origin of overpressures in sedimentary basins," *Acta Petrolei Sinica*, vol. 38, no. 9, pp. 973–998, 2017.

[25] H. Cao, J. J. Gong, and G. F. Wang, "The cause of overpressure and its relationship with reservoir forming," *Natural Gas Geoscience*, vol. 17, no. 3, pp. 422–425, 2006.

[26] Z. H. Jin and S. E. Johnson, "Primary oil migration through buoyancy driven multiple fracture propagation: oil velocity and flux," *Geophysical Research Letters*, vol. 35, no. 9, pp. 250–258, 2008.

[27] B. Durand, "Present trends in organic geochemistry in research on migration of hydrocarbons," in *Advances in Organic Chemistry*, pp. 117–128, John Wiley, New York, 1983.

[28] B. E. Law and C. W. Spencer, "Abnormal pressure in hydrocarbon environments," *AAPG Memoir*, vol. 70, no. 1, pp. 1–11, 1998.

[29] X. J. Guo, "Research of periods and differences of Yingcheng Formation in Longfengshan subdepression, Changling fault depression, Songliao Basin," *Jilin Geology*, vol. 38, no. 4, pp. 34–39, 2019.

[30] M. C. Li and J. Li, "Dynamic trap: a main action of hydrocarbon charging to form accumulations in low permeability-tight reservoir," *Acta Petrolei Sinica*, vol. 31, no. 5, pp. 718–722, 2010.

[31] Z. L. Pang, S. Z. Tao, and Q. Zhang, "Simulation experiments of tight oil secondary migration driving force and resistance: a case study of Jurassic oilfield in middle Sichuan basin," *Journal of China University of Mining & Techiology*, vol. 45, no. 4, pp. 754–764, 2016.

[32] Z. Q. Feng, S. Zhang, and Z. H. Feng, "Discovery of "enveloping surface of oil and gas overpressure migration" in the Songliao Basin and its bearings on hydrocarbon migration and accumulation mechanisms," *Science China (Earth Science)*, vol. 55, no. 12, pp. 2005–2017, 2012.